中国光学（中英文） Chinese Optics 核心期刊

Widely-wavelength-tunable brillouin fiber laser with improved optical signal-to-noise ratio based on parity-time symmetric and saturable absorption effect

LIU Yi, JIANG Kai, FANG Xin-yue, YOU Ya-jun, HE Wen-jun, HOU Jia-xin, HAN Xue-feng, CHOU Xiu-jian

Citation:
LIU Yi, JIANG Kai, FANG Xin-yue, YOU Ya-jun, HE Wen-jun, HOU Jia-xin, HAN Xue-feng, CHOU Xiu-jian. Widely-wavelength-tunable brillouin fiber laser with improved optical signal-to-noise ratio based on parity-time symmetric and saturable absorption effect[J]. *Chinese Optics*, 2024, 17(5): 1244-1253. doi: 10.37188/CO.EN-2024-0016
刘毅, 江恺, 房新岳, 游亚军, 贺文君, 侯甲欣, 韩学锋, 丑修建. 基于宇称时间对称与饱和吸收效应的宽可调谐高光信噪比布里渊光纤激光器[J]. 中国光学, 2024, 17(5): 1244-1253. doi: 10.37188/CO.EN-2024-0016

View online: https://doi.org/10.37188/CO.EN-2024-0016

文章编号 2097-1842(2024)05-1244-10

Widely-wavelength-tunable brillouin fiber laser with improved optical signal-to-noise ratio based on parity-time symmetric and saturable absorption effect

LIU Yi[1*], JIANG Kai[1], FANG Xin-yue[1], YOU Ya-jun[2], HE Wen-jun[1,3], HOU Jia-xin[1], HAN Xue-feng[1], CHOU Xiu-jian[1*]

(1. *State Key Laboratory of Dynamic Measurement Technology*, *School of Instrument and Electronics*, *North University of China*, *Taiyuan* 030051, *China*;
2. *School of Aerospace Engineering*, *North University of China*, *Taiyuan* 030051, *China*;
3. *Shanxi Province Key Laboratory of Quantum Sensing and Precision Measurement*, *North University of China*, *Taiyuan* 030051, *China*)

* *Corresponding author*, *E-mail*: *liuyi*28@163.*com*; *chouxiujian@nuc.edu.cn*

Abstract: A widely-wavelength-tunable Brillouin fiber laser (BFL) with improved optical signal-to-noise ratio (OSNR) based on parity-time (PT) symmetric and saturable absorption (SA) effect is present. This novel BFL realizes PT symmetry and SA effect through polarization-maintaining erbium-doped fiber (PM-EDF) Sagnac loop, which is composed of a PM-EDF, a coupler and two polarization controllers (PCs). By using the inherent birefringence characteristic of PM-EDF, two feedback loops in orthogonal polarization state are formed when the Strokes signal in injected. One of these loops provides gain in the clockwise direction with in the Sagnac loop, while the other loop generates loss in the counterclockwise direction. By adjusting the PCs to control the polarization state of the PM-EDF, a single-longitudinal-mode (SLM) BFL can be achieved, as the PT symmetry is broken when the SA participating stimulated Brillouin scattering (SBS) gain and loss are well-matched and the gain surpasses the coupling coefficient. Compared to previous BFLs, the proposed BFL has a more streamlined structure and a wider wavelength tunable range, at the same time, it is not being limited by the bandwidth of the erbium-doped fiber amplifier while still maintaining narrow linewidth SLM output. Additionally, thanks to SA effect of the PM-EDF, the PT symmetric SBS gain contract is enhanced, resulting in a higher optical signal-to-noise (OSNR). The experimental results show that the laser has a wide tunable range of 1 526.088 nm to 1 565.498 nm, an improved OSNR of 77 dB, and a fine linewidth as small as 140.5 Hz.

Key words: Brillouin fiber laser; widely-wavelength-tunable; parity-time symmetric; high OSNR; narrow linewidth

收稿日期:2024-06-05; **修订日期**:2024-07-03

基金项目:国家自然科学基金(No. U23A20639, No. U2341210, No. 62371426); 山西省中央引导地方科技发展资金项目(No. YDZJSX2022B005)

Supported by the National Natural Science Foundation of China (No. U23A20639, No. U2341210, No. 62371426); Central Guidance on Local Science and Technology Development Fund of Shanxi Province (No. YDZJSX2022B005)

基于宇称时间对称与饱和吸收效应的宽可调谐高光信噪比布里渊光纤激光器

刘　毅[1*], 江　恺[1], 房新岳[1], 游亚军[2], 贺文君[1,3], 侯甲欣[1], 韩学锋[1], 丑修建[1*]
（1. 动态测试技术国家重点实验室 仪器与电子学院, 中北大学, 太原 030051;
2. 航空宇航学院, 中北大学, 太原 030051;
3. 山西省量子传感与精密测量重点实验室, 中北大学, 太原 030051）

摘要: 本文提出了一种基于宇称时间对称与饱和吸收效应的宽可调谐高光信噪比布里渊光纤激光器。这种新型布里渊光纤激光器是通过使用保偏掺铒光纤 Sagnac 环实现宇称时间对称和饱和吸收效应的。保偏掺铒光纤 Sagnac 环是由一个保偏掺铒光纤、一个耦合器和两个偏振控制器构成的。利用保偏掺铒光纤固有的双折射特性, 在注入 Stokes 信号时形成两个处于正交偏振态的反馈环。其中一个环路在 Sagnac 环内提供顺时针方向的增益, 而另一个环路在逆时针方向产生损耗。当饱和吸收效应参与的受激布里渊散射增益和损耗相平衡, 并且增益值大于耦合系数时, 由于宇称时间对称性被破坏, 通过调整偏振控制器改变保偏掺铒光纤的偏振态, 可获得单纵模布里渊光纤激光器。与以往的布里渊光纤激光器相比, 本文提出的激光器具有更精简的结构和更宽的波长可调范围, 且不受掺铒光纤放大器带宽的限制, 同时仍保持窄线宽单纵模输出。此外, 由于保偏掺铒光纤的饱和吸收效应, 提高了宇称时间对称受激布里渊散射增益对比度, 因此获得了更高的光信噪比。实验结果表明, 该激光器具有 1 526.088 ~ 1 565.498 nm 宽可调范围、77 dB 光信噪比和 140.5 Hz 线宽。

关　键　词: 布里渊光纤激光器; 波长可调; 宇称时间对称; 高光信噪比; 窄线宽
中图分类号: O437.2　　**文献标志码:** A　　**doi:** 10.37188/CO.EN-2024-0016

1　Introduction

Stimulated Brillouin Scattering (SBS) is a phenomenon in laser physics and nonlinear optics, which results from the coupling of coherent light and sound. This process has a rich history and has been extensively studied[1-3]. Brillouin fiber laser (BFL) makes use of low noise and narrow bandwidth characteristic of Brillouin amplification, has been widely used in various applications, such as optical communication systems[4-6], distributed/point fiber sensing[7-8], and optical bistability[9-11]. The single-longitudinal-mode (SLM) and narrow linewidths BFL has been achieved utilizing a variety of methods. For example, a BFL with a 20 Hz ultra-narrow linewidth based on a large mode-volume (2 meters) optical fiber resonator, has been demonstrated[12]. Additionally, by confining a stabilized self-injected distributed feedback (DFB) laser diode into a high Q-factor 11-meter-long fiber ring cavity, the BFL's linewidth has been narrowed to 400 Hz[13]. Injection laser locking and composite cavity techniques can also be used to reduce the SBS gain spectrum linewidth. However, the erbium-doped fiber amplifier's bandwidth imposes a restriction on BFL's tunability[14]. For BFL with longer cavity[15], SLM output is challenging due to mode competition and higher optical signal-to-noise ratio (OSNR) requires higher pump intensity. The use of compound cavity and ultra-narrow bandwidth filter undoubtedly increases the operation difficulty and implementation cost.

The concept of Parity-Time (PT) symmetry, derived from a quantum mechanical principle, has garnered substantial attention from researchers in the fields of optics and beyond[16-18]. The ability to effectively select modes is a crucial attribute of PT symmetry, and has been applied to long cavity BFLs, yielding a SLM output. The use of PT symmetry in semiconductor or fiber lasers as well as optoelectronic oscillators (OEOs) has become more

and more popular in recent years. To achieve OEOs under SLM status, researchers have employed various techniques, such as constituting a dual-polarization loop incorporating a $LiNbO_3$ phase modulator (PM) at 2 to 12 GHz tunable frequencies range[19], utilizing a single Sagnac loop to construct two interconnected feedback loops based on spatial wavelength[20], and constructing two same hybrid optoelectronic loops primarily composed of a common dual-parallel Mach-Zehnder modulator (DP-MZM) and a photodetector, with a 60 dB side mode suppression ratio (SMSR)[21]. Another frequently used method for mode selection in fiber lasers is PT symmetry. For instance, in Ref. [22], PT symmetry was leveraged to realize a fiber laser with 129 kHz 3-dB linewidth, using optical polarization diversity between two subspaces of a single spatial unit. In the design of PT symmetry lasers, fiber Bragg gratings (FBGs) are also broadly utilized. The development of a resonator with two opposing PT symmetry FBGs has enabled the fabrication of a SLM laser with a linewidth of 8.667 kHz[23]. In order to accomplish PT symmetry in a fiber ring laser, a single Sagnac fiber loop was used, yielding a 41.9 dB SMSR and 390 Hz linewidth[24]. However, it has been reported that BFLs based on PT symmetry have limited tunability and OSNR, with a mere 1 nm tunability range and 65 dB OSNR[25-26]. Thus, it is imperative to further investigate various PT symmetric BFL structures and conduct comprehensive assessments of their performance in order to expand the adjustable range and OSNR.

In this paper, we present a widely-wavelength-tunable BFL with improved OSNR based on PT symmetric and saturable absorption (SA) effect by polarization-maintaining erbium-doped fiber (PM-EDF) Sagnac loop. Furthermore, we carry out experiment to verify its performance.

2 Principle

2.1 Experimental device

The experimental configuration for the proposed widely-wavelength-tunable BFL is depicted in Fig. 1. A tunable laser source (TLS: PPCL 550), characterized by a 10 kHz linewidth and a wavelength-tunable range of 1 526 to 1 565.41 nm, is employed as the pump for the BFL and is fed into the 10 km single-mode fiber (SMF) via a circulator (Cir1) and PC1. Upon surpassing the SBS threshold, the pump elicits the generation of Stokes light through SBS. The Stokes light then circulates clockwise in the ring resonator, which is comprising of the 90/10 OC1, Cir1, Cir2, 10 km SMF, and the PM-EDF Sagnac loop. Subsequently, the Stokes light is launched into the PM-EDF Sagnac loop through Cir2. The PM-EDF Sagnac loop comprises a 50/50 optical coupler (OC3), a PM-EDF that spans 50 cm in length, and two polarization controllers (PC2 and PC3). The inherent birefringence of the PM-EDF enables the formation of two mutually coupled loops, one with SBS gain and the other with loss of SA participation, arising from the splitting and clock-wise/counterclockwise motion of the incident light. By adjusting the PCs control the polarization state of the injected Stokes light, the SA participating SBS gain and the loss of the loops corresponding to the clockwise and counterclock-wise light can be precisely regulated. When the light waves go through the same PM-EDF Sagnac loop, the two loops lengths are nearly similar. The PT symmetry is broken when the SA participating SBS gain and loss are well matched and the gain exceeds the coupling coefficient, the output of a BFL is triggered in turn. The SA can enhance SBS gain contrast value, leading to a higher OSNR for the laser[25-26]. The Stokes wave is then fed through Cir2 into the ring cavity and passes through many clockwise roundtrips. The Stokes wave is divided two beams by 90/10 OC1, 90% of the divided Stokes light circulates in the ring resonator, and 10% is used as the output laser for the BFL. The output of widely-wavelength-tunable BFL is split into two light by the 90/10 OC2. An optical spectrum analyzer (OSA) with 0.01 nm resolution is used to monitor the SLM laser in one beam, while the other beam is converted into an electrical signal

by a photodetector (PD) and detected by an electrical spectrum analyzer (ESA) with a resolution of 1 Hz.

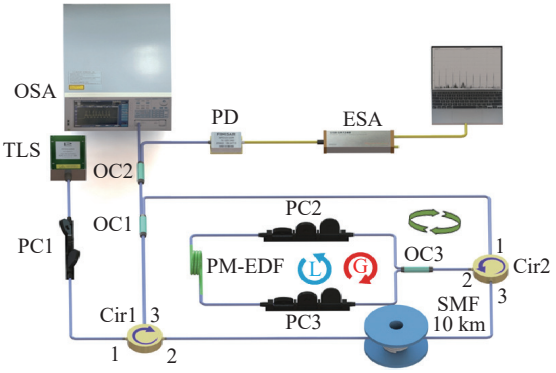

Fig. 1　Experimental setup. TLS: tunable laser source; Cir: circulator; PC: polarization controllers; OC: optical coupler; SMF: single-mode fiber; ESA: electrical spectrum analyzer; PM-EDF: polarization maintaining erbium-doped fiber; PD: photodetector; OSA: optical spectrum analyzer.

2.2　Free spectral range

The SBS effect causes a frequency shift from the center frequency f_c to $f_c - f_B$, which occurs within the 10-km SMF after the pump wave injected into the tunable laser source via the circulator. The magnitude of the Brillouin frequency shift f_B is defined as $(2V_A/c)v_p$, where V_A represents the acoustic velocity in the medium, c denotes the velocity of light, and v_p represents the optical frequency of the pump beam. It is worth noting that when the wavelength is 1549.955 nm, f_B is approximately 10.735 GHz. The Brillouin gain spectrum exhibits the linewidths of Δf_B = 20 MHz.

Additionally, the free spectral range (FSR) for the 10 km SMF is also specified as well[6],

$$\mathrm{FSR} = \frac{c}{nL_m} \quad , \qquad (1)$$

where L is the length of ring resonator. In Fig. 2(a) (color online), n equals to the effective index of the fiber, is 1.468, and L denoting the length of the ring cavity, the widely-wavelength-tunable BFL's FSR is determined to be 21 kHz.

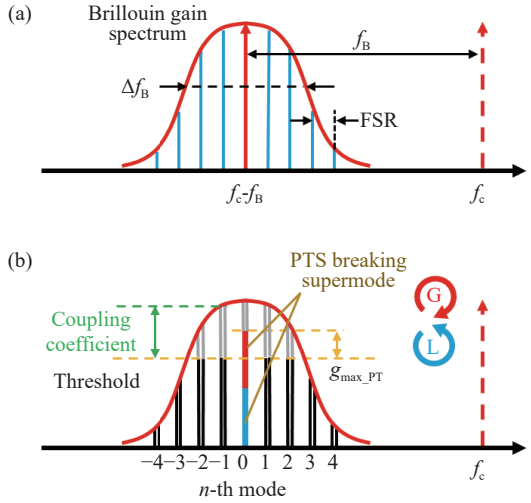

Fig. 2　The foundational concept behind the BFL based on PT symmetric and SA effect. (a) The occurrence of Stimulated Brillouin Scattering in the optical spectrum. (b) The mode selection operational principle when the PT symmetry breaking occurs within the PT-symmetric BFL

2.3　The SA effect and PT symmetry

The SA coefficient in the EDF may be written as[27]:

$$a_n = \frac{a_l}{1 + I_n / I_{\mathrm{sat}}} \quad , \qquad (2)$$

where represents the linear absorption coefficient of the medium, and denotes the saturation intensity. The inherent birefringence of PM-EDF is utilized to form two equivalent loops constituting the PT symmetry, with one loop exhibiting gain from SBS and the other displaying loss. The following is a representation of the coupling equations for the modes inside the cavity in the time domain[28]:

$$\frac{\mathrm{d}}{\mathrm{d}t}\begin{bmatrix} A_n \\ B_n \end{bmatrix} = \begin{bmatrix} -i\omega_n + g'_{B\_A_n} & ik_n \\ ik_n & -i\omega_n + g'_{B\_B_n} \end{bmatrix}\begin{bmatrix} A_n \\ B_n \end{bmatrix}. \qquad (3)$$

The n-th modes' amplitudes in the SA participating SBS gain and loss loops, expressed as A_n and B_n, respectively. With the lacking PT symmetry, the longitudinal modes localized eigenfrequency are affected, designated as ω_n. The SA participating SBS gain and loss coefficients of the n-th mode, defined as $g'_{B\_A_n} = g_{B\_A_n} - a_n$ and $g'_{B\_B_n} = g_{B\_B_n} - a_n$. It's a result of the interaction between the SBS gain and the

inherent loss of the laser cavity in our system. In the PT symmetric setup, for the n-th mode, another key determinant is the coupling coefficient represented by k_n between the two coupled loops. The eigenfrequencies of the PT-symmetric system may be derived by solving the Eq. (4).

$$\omega_n^{(1,2)} = \omega_n + i\frac{g'_{B\_A_n}+g'_{B\_B_n}}{2} \mp \sqrt{k_n^2-\left(\frac{g'_{B\_A_n}-g'_{B\_B_n}}{2}\right)^2}. \tag{4}$$

Assuming that the desired PT-symmetric condition can be met by adjusting the phase compensators, then a SLM output for the designated mode can be obtained, we have $g'_{B\_A_n}=-g'_{B\_B_n}=g'_{B_n}$. Eq. (4) can be written as

$$\omega_n^{(1,2)} = \omega_n \mp \sqrt{k_n^2-g'^2_{B_n}} \quad . \tag{5}$$

Under the conditions that $g'_{B_n} < k_n$, the PT-symmetric system operates within an unbroken regime, resulting in the frequency division of a specific mode. Conversely, if $g'_{B_n} > k_n$, the PT-symmetry is deemed broken and a conjugate pair of modes experiences a discernible deviation; one mode experiences SBS gain while the other encounters a loss, while the remaining modes remain unaffected, as demonstrated in Fig. 2(b).

Additionally, in a conventional BFL, the SLM operation can be achieved as long as the primary mode's SBS gain, specifically, the 0-th mode's g_{B_0}, surpasses the oscillation threshold while the SBS gain of the other modes remains below the threshold. Under such circumstances, the maximal contrast of SBS gain is measured as follows:

$$g'_{\max} = g'_{B_0} - g'_{B_1} \quad . \tag{6}$$

Under PT symmetry, the gain difference between $g'_{B_0} = g_{B_0} - a_0$ and g'_{B_1} can be calculated by Eq. (7). This results in a significantly greater gain contrast as compared to the regular BFL scenario, which enhances the stability of the SLM laser. The gain difference is calculated as follows:

$$g'_{\max\_PT} = \sqrt{g'^2_{B_0} - g'^2_{B_1}} \quad . \tag{7}$$

The measure of the improvement in mode selection, known as the SBS gain enhancement or gain contrast ratio, is determined by comparing the gain difference between a conventional laser source and a laser source that possesses PT symmetry. This ratio is given by Eq. (8) and serves as a useful metric for assessing the PT-symmetric laser's performance in comparison to traditional laser.

$$G' = \frac{g'_{\max\_PT}}{g'_{\max}} = \sqrt{\frac{g'_{B_0}/g'_{B_1}+1}{g'_{B_0}/g'_{B_1}-1}} \quad . \tag{8}$$

Thus, with the utilization of the PT-symmetric configuration, the SLM operation can achieve a higher SBS gain contrast, resulting in a higher OSNR lasing.

2.4 The linewidth of the BFL based on PT symmetric and SA effect

The BFL is renowned for its exceptional narrow linewidth characteristic, which is able to transform a pump wave with broad linewidth into a Brillouin Stokes wave with a remarkably narrow linewidth. There exist two methods for determining the linewidth of BFL.

The linewidths of the BFL, Δf_B, and the pump light, Δv_p, have a proportional relationship that may be written as follows[29]:

$$\Delta f_B = \frac{\Delta v_p}{\left(1+\pi\Delta v_B/\left(-\frac{c\ln R}{nL}\right)\right)^2} \quad . \tag{9}$$

With the SBS gain spectrum intrinsic linewidth being Δv_B = 20 MHz, and the amplitude feedback coefficient of the widely-wavelength-tunable BFL being $R = 0.5 \times 0.9 = 0.45$, Eq. (9) reveals that, given a pump light linewidth of Δv_p = 10 kHz, the linewidth of the BFL, $\Delta f_B = 6.910 \times 10^{-4}$ Hz.

Lasers with wide linewidths, such as semiconductor lasers, He-Ne lasers, fiber DFB lasers, and fiber DBR lasers, are characterized by their short cavity lengths. The Schawlow-Towns linewidth limit, which represents the maximum linewidth of the laser, is specified by[30]:

$$\Delta f_B = \frac{2\pi(\Delta v_c)^2 h f_c}{P_0} \quad . \qquad (10)$$

The FWHM is represented by $\Delta v_c = cL_c/2\pi L$, where L_c denotes the net loss of the cavity, P_0 signifies the output intensity, and h symbolizes Planck's constant. For a fiber ring laser operating at a wavelength of λ = 1 549.996 nm with a 10 km long resonator, a net loss of 0.45, and an output intensity of 0.005 mW, the calculated linewidth limit is extremely small, at $\Delta f_B = 2.47 \times 10^{-15}$ Hz.

The narrow linewidth of BFL, resulting from its capability to convert wide linewidth pump light into Brillouin Stokes light, is a remarkable attribute. The linewidth of BFL can be calculated through two methods. The equation (9) provides the proportional correlation between the linewidths of the pump wave Δv_p and the BFL Δf_B. Here, the calculated value of Δf_B is 6.910×10^{-4} Hz, while the linewidth of the pump light is determined to be 10 kHz. Although, the theoretical BFL's linewidth is immensely narrow, but the actual linewidth may be wider due to the inherent noise and instability of the setup.

3　Results and discussion

3.1　Wavelength tunability and OSNR measurements of the BFL based on PT symmetric and SA effect

The proposed BFL based on PT symmetric and SA effect was evaluated experimentally by utilizing the setup illustrated in Fig. 1. The pump wave at 1 549.996 nm emitted by the TLS, possessing a 10 kHz 3-dB linewidth in the experiment. Fig. 3(a) (color online) depicts the output optical spectra of the BFL and the TLS pump light, showcasing a remarkable OSNR of 77 dB. The output intensity of the BFL in relation to the pump intensity is illustrated in Fig. 3(b) (color online), where the pump intensity was measured at the TLS and the BFL output intensity was recorded at the 10% port of the OC1. The maximum 10 mW output intensity was achieved while preserving stable single-frequency operation.

The output wavelength of the BFL perfectly aligns with the Brillouin frequency shift of the pump laser, thereby allowing for the control of the lasing wavelength, resulting in a wide tunability range. The ability to adjust the output wavelength of the TLS within the range of 1 526 to 1 565.41 nm, enables the wavelength tuning of the BFL between 1 526.088 to 1 565.498 nm, as demonstrated in Fig. 4 (color online). The figure presents the stable tuning of the BFL's optical spectra within the frequency range of 1 528−1 564 nm, with a tuning step size of approximately 2 nm, all while preserving a high OSNR of 77 dB, which is increased by 12 dB with respect to the general PT symmetric BFL[25-26]. This design not only has higher OSNR but also has a broader tunable range, as compared to existing BFL designs[31]. Furthermore, this design is not limited by the bandwidth of the erbium-doped fiber amplifier (EDFA).

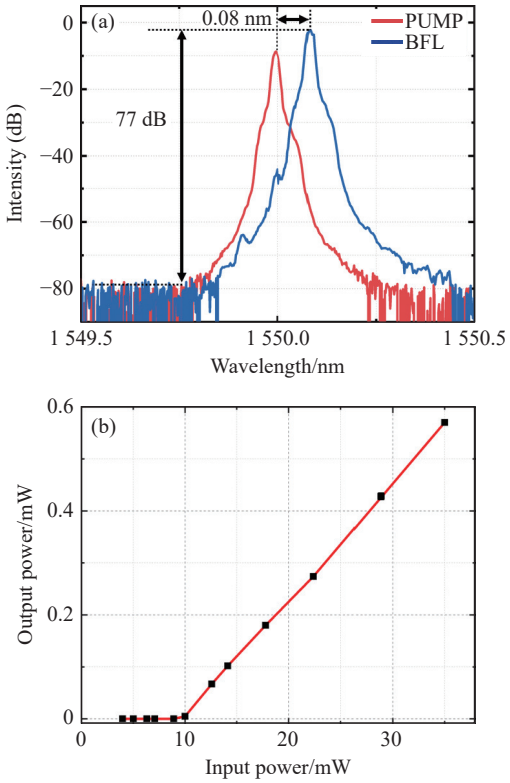

Fig. 3　Measured optical spectrum. (a) The optical spectrum of the BFL and 1 550 nm pump wavelength and (b) the threshold curve between the pump intensity and BFL output intensity

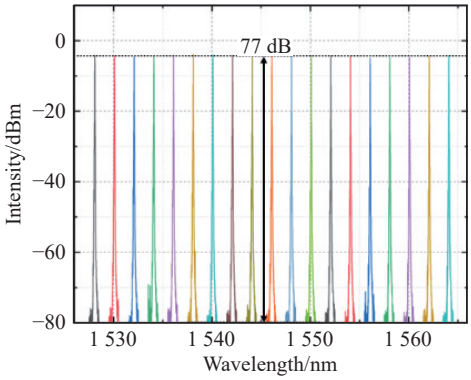

Fig. 4 The wavelength tunability measurement results of the BFL based on SA effect and PT symmetric

3.2 Single longitudinal mode of the BFL based on PT symmetric and SA effect

As depicted in Fig. 5 (color online), the spectrum of the frequency beat signal at the PD output when pump wavelength is set to 1 550 nm is measured. The attainment of PT symmetry and SLM lasing are dependent upon the adjustment of SA participating SBS gain and loss to be matched, as evidenced by the generation of multiple frequency beat signals at 100 kHz to 4 MHz frequency range when PT symmetry is not achieved, as depicted in Fig. 5(a). Conversely, by precisely tuning the phase compensators PC1 and PC2 to achieve a well-matched SA participating SBS gain and absorption loss, exceeding the coupling coefficient and thus breaking PT symmetry, SLM BFL is achieved, as shown in Fig. 5(b). While, in Fig. 5(c) and (d), the zoomed-in view-ports of the unbroken and broken PT-symmetry at the frequency range of 100−300 kHz are presented, with a maximum SMSR of 16 dB corresponding to an FSR of 21 kHz, which, according to Eq. (1), corresponds to a cavity length of 10 km cavity length. These measurement results are consistent with the theoretical predictions. Similarly, the zoomed-in view-ports of the unbroken and broken PT-symmetry at 300−500 kHz frequency range are shown in Fig. 5(e). It can be seen that the maximum SMSR is 14 dB. Furthermore, Fig. 5(f) illustrates the maximum SMSR of 14 dB between unbroken and broken PT-symmetry at 500−700 kHz frequency range.

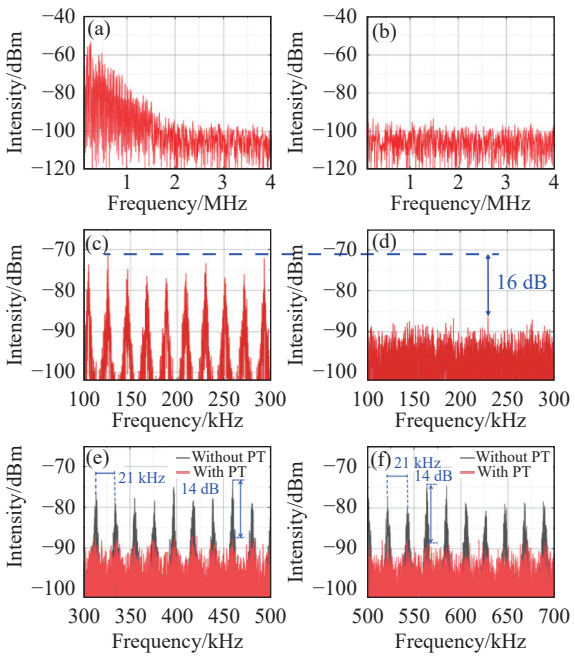

Fig. 5 The spectral analysis results of the frequency beat signals emitted from the PD. (a) Unbroken PT-symmetry and (b) broken PT-symmetry with their magnified view under 0−4 MHz frequency range; (c) and (d) are enlarged views at 100−300 kHz respectively; (e) and (f) present a comparative diagram of the measured spectra, demonstrating the effects of PT-symmetry under 300−500 kHz and 500−700 kHz frequency ranges respectively

3.3 Linewidth measurement of the BFL based on PT symmetric and SA effect

Fig. 6 shows the schematic diagram of the linewidth measurement setup to determine the linewidth of the BFL based on PT symmetric and SA effect. The output of the TLS is divided into two beams by a 50/50 OC1, which acting as the pump. In the upper branch, a second BFL is established, consisting of a Cir1, 10-km SMF and a 90/10 OC2. The pump output, which exceeds the SBS threshold, is injected into the 10 km SMF via Cir1 and generates Stokes light as a result of SBS. This Stokes light undergoes numerous CCW roundtrips, resulting in periodic resonances within the ring cavity, each of which possess a linewidth that is remarkably narrow. The laser output is then acquired via 10% of OC3 and combined with the output of the BFL based on PT symmetric and SA effect via a 1∶1 OC4. By detecting the beat frequency between the

two BFLs via a PD, the laser linewidth can be measured with an ESA. The electrical spectrum at the PD output is depicted in Fig. 7. The theoretical linewidth of BFL, according to Eq. (8), is about 10^{-8} Hz, surpassing the ESA measurement accuracy with 1 Hz. The linewidth under the -20 dB intensity point was determined to be 2.81 kHz, equating to 140.5 Hz 3-dB linewidth.

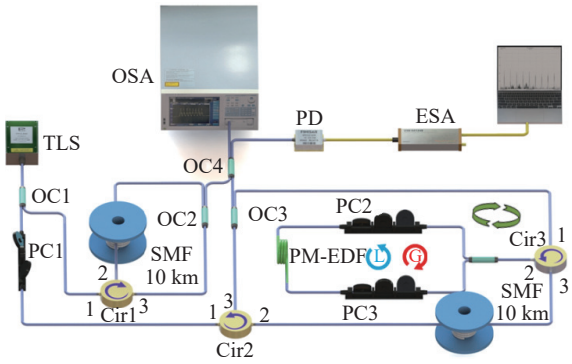

Fig. 6　The linewidth measurement setup of the BFL based on PT symmetric and SA effect

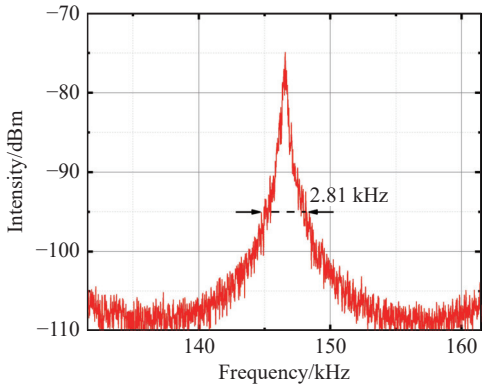

Fig. 7　The linewidth measurement results of the BFL under the -20 dB intensity point

4　Conclusion

In conclusion, we have proposed and validated experimentally a BFL based on PT symmetric and SA effect with the unique characteristics of widely tunable wavelengths and high OSNR, while still maintaining narrow linewidth SLM lasing. To attain PT symmetry, we utilized a PM-EDF Sagnac loop composed of two polarization controllers and a PM-EDF. After stimulating SBS gain in the 10 km SMF with the pump light, the Stokes wave was injected into the Sagnac loop. The inherent birefringence of the PM-EDF generated two interconnected feedback loops for polarized orthogonally wave, with one loop experiencing SBS gain and the other experiencing SBS loss. The gain and loss of SBS could be regulated precisely by varying polarization state of the injected Stokes wave. When the gain and loss of SBS involving SA were perfectly matched and the gain exceeded the coupling coefficient, PT symmetry was broken, resulting in a high coherent BFL. By adjusting center wavelength of the the pump light, the output wavelength of BFL could be tuned. It is worth mentioning that this design does not require an EDFA to amplify the pump intensity, thus, the tunability of this BFL is not limited by EDFA bandwidth, allowing for a wider tuning range of wavelengths. Furthermore, due to the advantage of SA in PM-EDF, there are a bigger gain contrast value and a higher OSNR. The wavelength of the BFL was set between 1 526.088 to 1 565.498 nm, and its OSNR is high, reaching 77 dB. Our experiments demonstrate 140.5 Hz linewidth of the BFL based on PT symmetric and SA effect, with a measured linewidth of 2.81 kHz at the -20 dB intensity point. With its advantages of widely tunable wavelengths and high OSNR, this design holds great potential for many application fields such as optical bistablity, ultrahigh-coherent optical communication and optical fiber sensing.

References:

[1] BRILLOUIN L. Diffusion de la lumière et des rayons X par un corps transparent homogène[J]. *Annales de Physique*, 1922, 9(17): 88-122.

[2] MANDELSTAM L I. Light scattering by inhomogeneous media[J]. *Zh Russ Fiz-Khim Ova*, 1926, 58: 381-391.

[3] GARMIRE E. Perspectives on stimulated Brillouin scattering[J]. *New Journal of Physics*, 2017, 19(1): 011003.

[4] AL-MASHHADANI M K S, AL-MASHHADANI T F, GOKTAS H H. Broadly tunable 40 GHz Brillouin frequency

spacing multiwavelength Brillouin–Erbium fiber laser for DWDM[J]. *Optics Communications*, 2019, 451: 116-123.

[5] AL-MANSOORI M H, AL-SHERIYANI A, YOUNIS M A A, *et al*.. Widely tunable multiwavelength Brillouin-erbium fiber laser with triple Brillouin-shift wavelength spacing[J]. *Optical Fiber Technology*, 2018, 41: 21-26.

[6] WANG L Y, LIU Y, YOU Y J, *et al*.. Microwave photonic filter with a sub-kHz bandwidth based on a double ring Brillouin fiber laser[J]. *Optics Letters*, 2022, 47(16): 4143-4146.

[7] BASTIANINI F, DI SANTE R, FALCETELLI F, *et al*.. Optical fiber sensing cables for Brillouin-based distributed measurements[J]. *Sensors*, 2019, 19(23): 5172.

[8] XU Y P, LU P, BAO X Y. Compact single-end pumped Brillouin random fiber laser with enhanced distributed feedback[J]. *Optics Letters*, 2020, 45(15): 4236-4239.

[9] LIU Y, SHANG Y, YI X G, *et al*.. Triple Brillouin frequency spacing Brillouin fiber laser sensor for temperature measurement[J]. *Optical Fiber Technology*, 2020, 54: 102106.

[10] SHANG Y, GUO R R, LIU Y, *et al*.. Managing Brillouin frequency spacing for temperature measurement with Brillouin fiber laser sensor[J]. *Optical and Quantum Electronics*, 2020, 52(4): 211.

[11] ZHU K Y, HE J Y, CHANG K, *et al*.. The multi-wavelength Brillouin laser based on highly nonlinear fiber[J]. *Proceedings of SPIE*, 2022, 12169: 1216935.

[12] LOH W, YEGNANARAYANAN S, O'DONNELL F, *et al*.. Ultra-narrow linewidth Brillouin laser with nanokelvin temperature self-referencing[J]. *Optica*, 2019, 6(2): 152-159.

[13] AHMAD H, RAZAK N F, ZULKIFLI M Z, *et al*.. Ultra-narrow linewidth single longitudinal mode Brillouin fiber ring laser using highly nonlinear fiber[J]. *Laser Physics Letters*, 2013, 10(10): 105105.

[14] PARVIZI R, AROF H, ALI N M, *et al*.. 0.16 nm spaced multi-wavelength Brillouin fiber laser in a figure-of-eight configuration[J]. *Optics & Laser Technology*, 2011, 43(4): 866-869.

[15] OU ZH H, BAO X Y, LI Y, *et al*.. Ultranarrow linewidth Brillouin fiber laser[J]. *IEEE Photonics Technology Letters*, 2014, 26(20): 2058-2061.

[16] BENDER C M, BOETTCHER S. Real spectra in non-Hermitian Hamiltonians having *P T* symmetry[J]. *Physical Review Letters*, 1998, 80(24): 5243-5246.

[17] ÖZDEMIR Ş K, ROTTER S, NORI F, *et al*.. Parity–time symmetry and exceptional points in photonics[J]. *Nature Materials*, 2019, 18(8): 783-798.

[18] EL-GANAINY R, MAKRIS K G, KHAJAVIKHAN M, *et al*.. Non-Hermitian physics and PT symmetry[J]. *Nature Physics*, 2018, 14(1): 11-19.

[19] LI P, DAI ZH, FAN ZH Q, *et al*.. Parity–time-symmetric frequency-tunable optoelectronic oscillator with a single dual-polarization optical loop[J]. *Optics Letters*, 2020, 45(11): 3139-3142.

[20] ZHANG J J, LI L ZH, WANG G Y, *et al*.. Parity-time symmetry in wavelength space within a single spatial resonator[J]. *Nature Communications*, 2020, 11(1): 3217.

[21] ZHANG J J, YAO J P. Parity-time–symmetric optoelectronic oscillator[J]. *Science Advances*, 2018, 4(6): eaar6782.

[22] LI L ZH, CAO Y, ZHI Y Y, *et al*. . Polarimetric parity-time symmetry in a photonic system[J]. *Light*: *Science & Applications*, 2020, 9: 169.

[23] ZHU Y Y, ZHAO Y S, FAN J H, *et al*.. Modal gain analysis of parity-time-symmetric distributed feedback lasers[J]. *IEEE Journal of Selected Topics in Quantum Electronics*, 2016, 22(5): 1500207.

[24] DAI ZH, FAN ZH Q, LI P, *et al*.. Widely wavelength-tunable parity-time symmetric single-longitudinal-mode fiber ring laser with a single physical loop[J]. *Journal of Lightwave Technology*, 2021, 39(7): 2151-2157.

[25] LIU Y, WANG L Y, XU X, *et al*.. Narrow linewidth parity-time symmetric Brillouin fiber laser based on a dual-polarization cavity with a single micro-ring resonator[J]. *Optics Express*, 2022, 30(25): 44545-44555.

[26] LIU Y, WANG L Y, YOU Y J, *et al*.. Single longitudinal mode parity-time symmetric Brillouin fiber laser based on lithium niobate phase modulator sagnac loop[J]. *Journal of Lightwave Technology*, 2023, 41(5): 1552-1558.

[27] LIU Y, GUO R R, ZHAO J J, *et al*.. An EDFA-gain equalizer based on a Sagnac loop with an unpumped erbium-doped fiber[J]. *Journal of Lightwave Technology*, 2021, 39(13): 4496-4502.

[28] MAKRIS K G, EL-GANAINY R, CHRISTODOULIDES D N, *et al*.. Beam dynamics in *P T* symmetric optical lattices[J]. *Physical Review Letters*, 2008, 100(10): 103904.

[29] DEBUT A, RANDOUX S, ZEMMOURI J. Linewidth narrowing in Brillouin lasers: theoretical analysis[J]. *Physical*

Review A, 2000, 62(2): 023803.

[30] POLLNAU M, EICHHORN M. Spectral coherence, Part I: passive-resonator linewidth, fundamental laser linewidth, and Schawlow-Townes approximation[J]. *Progress in Quantum Electronics*, 2020, 72: 100255.

[31] WANG G M, ZHAN L, LIU J M, *et al*.. Watt-level ultrahigh-optical signal-to-noise ratio single-longitudinal-mode tunable Brillouin fiber laser[J]. *Optics Letters*, 2013, 38(1): 19-21.

Author Biographic：

Liu Yi (1984—), male, born in Changzhi city, Shanxi province, Associate Professor. He obtained bachelor's and master's degrees from North University of China in 2007 and 2010, respectively, and Ph.D. from Tianjin University in 2014. He mainly engages in research on fiber lasers and fiber sensing. E-mail: liuyi28@163.com